High-Spin Radical Cations of a Dendritic Oligoarylamine

Yasukazu Hirao, Haruhiro Ino, Akihiro Ito,* and Kazuyoshi Tanaka[†]

Department of Molecular Engineering, Graduate School of Engineering, Kyoto University, Nishikyo-ku, Kyoto 615-8510, Japan, and CREST, Japan Science and Technology Agency (JST), Japan

Tatsuhisa Kato

Department of Chemistry, Josai University, 1-1 Keyakidai, Sakado, Saitama 350-0295, Japan

Received: October 11, 2005

A new dendritic oligoarylamine, *N*,*N*,*N*′,*N*′,*N*″,*N*″-hexakis[4-(di-4-anisylamino)phenyl]- 1,3,5-benzenetriamine (BTA) **2**, which contains a 1,3,5-benzenetriamine molecular unit as an potential precursor of a high-spin molecule and three oligoarylamine moieties as spin-carrying units surrounding the core BTA, has been prepared by the sequential palladium-catalyzed amination reactions. The redox property has been investigated by cyclic voltammetry, and the highly charged states up to the hexacation are accessible to **2**. The polycationic high-spin species have been generated by stepwise chemical oxidation, and the electronic structures have been examined in detail by the continuous wave (CW) and pulsed ESR spectroscopy in comparison with the previously studied **1**. The pulsed ESR technique enabled us to determine the definite spin multiplicity of the generated polycationic species of **2**. It was confirmed that the dominant oxidized species observed by the two- and three-electron oxidations were assigned to the spin triplet $\mathbf{2}^{2+}$ and the spin quartet $\mathbf{2}^{3+}$, respectively. Moreover, these high-spin polycationic species turned out to be far more stable as compared to **1**, and the isolation of $\mathbf{2}^{3+}$ as the $SbCl_6^-$ salt has been accomplished. The temperature dependence of the magnetic susceptibility for the $\mathbf{2}^{3+}(SbCl_6^-)_3$ salt revealed that the intramolecular ferromagnetic interaction exists in $\mathbf{2}^{3+}$, and moreover, the trication $\mathbf{2}^{3+}$ was found to be deformed in the solid state.

Introduction

Oligoarylamines have been intensively studied in recent years. They are widely used as hole-transport (HT) materials in organic electroluminescent (EL) devices owing to the facile generation of their radical cations and the stability of the generated hole carriers.[1−4] More fundamentally, partially oxidized triarylamine-based molecular systems were investigated as a typical example for purely organic mixed-valence compounds to elucidate the intramolecular hole-transfer processes,[5,6] and also, excitation energy transfer in triarylamine dendrimers was examined in conjunction with exploitation of artificial light-harvesting molecular systems.[7] In addition, aiming at the controlled charge transport, redox-gradient or redox-cascade systems have been pursued by incorporating several kinds of triarylamine units into their oligomeric and dendritic architectures.[8−11] Besides these interesting electronic properties, there has been considerable interest in arylamine-based magnetic materials,[12−15] and novel organic high-spin arylaminium radical cations have been prepared by taking advantage of their stable multi-redox properties.[16−23] In contrast to the HT case, the triarylamine moieties as spin-carrying units were isolated in order to avoid the formation of closed-shell electronic structures. In all these cases, it should be noted that the dendritic structural motif has often been used to give a new possibility for arranging the charge-transporting and/or spin-carrying units into suitable sites.

We recently described the synthesis of the star-shaped arylamine **1** and the electronic properties of the oxidized species.[16f] This molecule consists of a central 1,3,5-benzenetriyl moiety as an effective ferromagnetic coupling unit and peripherally substituted three arylamine moieties as spin-carrying units.

SCHEME 1

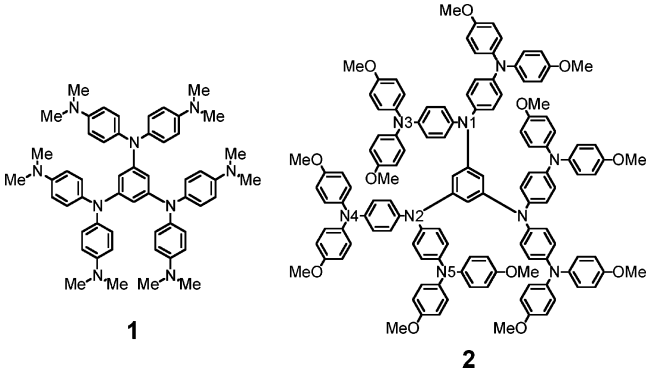

The latter arylamine moiety is known as the Bindschdler's green (BG) leuco base [4,4′-bis(dimethylamino)diphenylamine] and can be converted into an isolable semiquinone radical cation (BG^+) salt by one-electron oxidation. Electrochemical studies showed multi-redox behavior of **1**, and it enabled us to observe the spin preference of each oxidation state by stepwise chemical oxidation. The observed spin multiplicity of each oxidation state of **1** was confirmed to be consistent with the conventional π-topological rule for organic high-spin molecules.[24] In particular, upon three-electron oxidation, the generated trication $\mathbf{1}^{3+}$ was shown to be spin quartet tri(radical cation). However, unfortunately, the oxidized species were found to be unstable at ambient atmosphere.

In the present study, as an extension of **1**, we prepared a new dendritic oligoarylamine **2** (Scheme 1), to examine the spin states of the oxidized species of **2** in comparison with those of **1** on the basis of the electron spin resonance (ESR) and magnetic susceptibility measurements. Apparently, this oligoarylamine **2**

* Author for correspondence. E-mail: aito@scl.kyoto-u.ac.jp.
[†] Japan Science and Technology Agency (JST).

10.1021/jp0557924 CCC: $33.50
Published on Web 03/21/2006

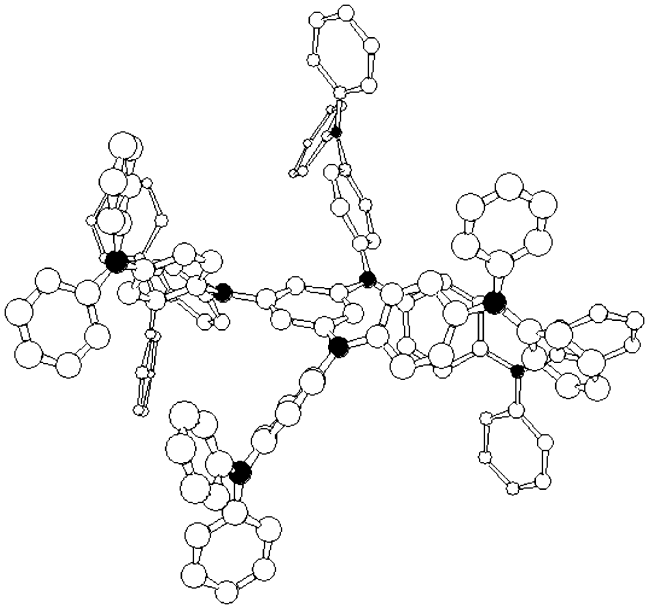

Figure 1. Optimized molecular structure of **2** under the D_3 symmetrical constraint calculated by the MNDO AM1 (modified neglect of diatomic overlap, Austin model 1) MO method. The nitrogen atoms are represented by the black-colored balls, and the hydrogen atoms are omitted for clarity.

can be regarded as a larger π-conjugated system than **1**, and therefore, we can expect that the extension of the π-conjugated system improves the stability of the charged states of **2**. In addition, substitution of a bulky dianisylamino group for a dimethylamino group leads to a considerable structural change due to steric hindrance in the periphery (Figure 1). It is interesting to examine how such a steric effect can influence the spin state in the oxidized species of **2**, as compared to that of **1**.

Experimental Section

General Methods. Commercial-grade regents were used without further purification. Solvents were purified, dried, and degassed following standard procedures. Elemental analyses were performed by the Center for Organic Elemental Microanalysis, Kyoto University. ^{1}H and ^{13}C NMR spectra were measured by a JEOL JNM-EX 400 FT-NMR spectrometer. Chemical shifts of NMR spectra are determined relative to tetramethylsilane (TMS) internal standard.

Electrochemical Measurements. Cyclic voltammograms were recorded in benzonitrile solution containing 0.1 M tetrabutylammonium perchlorate as a supporting electrolyte (room temperature, scan rate 100 mVs^{-1}) using an ALS/chi electrochemical analyzer model 612A with a three-electrode cell using a Pt disk (2 mm^2), a Pt wire, and an Ag/0.01 M $AgNO_3$ (MeCN) as the working, counter, and reference electrodes, respectively. All the reported redox potentials were calibrated against ferrocene/ferrocenium (Fc/Fc^+) redox couple.

ESR Measurements. ESR spectra were measured using a JEOL JES-RE-2X X-band spectrometer. Pulsed ESR measurements were carried out on a Bruker ELEXES E580 X-band FT ESR spectrometer. The electron spin transient nutation (ESTN) measurements were performed by the three-pulse sequence shown in Figure 2. The two-pulse ($\pi/2 - \pi$ pulses) electron spin−echo signal $S(t_1)$ was detected by increasing the width (t_1) of the nutation pulse. The observed signal $S(t_1, B_0)$ as a function of external magnetic field B_0 is converted into a nutation frequency $S(\omega_n, B_0)$ spectrum. The parameters used

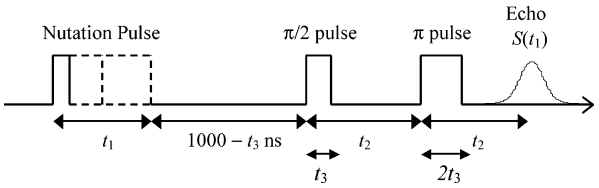

Figure 2. Pulse sequence used for the present electron spin transient nutation measurements.

for the measurements of **2** treated with 2 equiv of oxidant were $t_2 = 300$ ns and $t_3 = 8$ ns. On the other hand, those for the measurement of **2** treated with 3 equiv of oxidant were $t_2 = 400$ ns and $t_3 = 8$ ns.

Magnetic Susceptibility Measurements. Magnetic susceptibilities of the powder sample of $\mathbf{2}^{3+}(SbCl_6^-)_3$ salt were measured by a Quantum Design MPMS-5S SQUID magnetometer from 2 to 300 K under a constant magnetic field of 500 G. The raw data were corrected for both the magnetization of the sample holder alone and the diamagnetic contribution of the sample itself. The diamagnetic contribution was estimated by using Pascal's constants.

***N*,*N*-Bis(4-bromophenyl)amine (3).** In an ice-cooled 300 mL round-bottom flask was dissolved diphenylamine (3.918 g, 23.15 mmol) in chloroform (50 mL). To this solution, $TBABr_3$ (22.33 g, 46.31 mmol) in chloroform (100 mL) was added dropwise via an addition funnel over 4 h. The resulting mixture was then washed with a saturated aqueous solution of $NaHCO_3$ and then dried over $MgSO_4$. Evaporation of solvent and flash column chromatography on silica with 3:2 hexane/dichloromethane and recrystallization from hexane afforded pure **3** (6.920 g, 91%) as white needles: ^{1}H NMR ($CDCl_3$) δ 7.35 (d, $J = 8.7$ Hz, 4H), 6.91 (d, $J = 8.7$ Hz, 4H), 5.64 (bs, 1H); ^{13}C NMR ($CDCl_3$) δ 141.70, 132.30, 119.50, 113.38. Anal. Calcd for $C_{12}H_9N_1Br_2$: C, 44.07; H, 2.77; N, 4.28; Br, 48.87. Found: C, 44.00; H, 2.50; N, 4.13; Br, 48.73.

***N*-*tert*-Butoxycarbonyl-*N*,*N*-bis(4-bromophenyl)amine (4).** To a solution of di-*tert*-butyl dicarbonate (1.0 M) in THF (15.5 mL) was added *N*,*N*-bis(4-bromophenyl)amine (3.36 g, 10.3 mmol) and 4-(dimethylamino)pyridine (0.26 g, 2.1 mmol), and the mixture was heated to reflux for 3 h with stirring. After cooling, evaporation of the solvent and recrystallization from hexane afforded pure **4** (3.95 g, 90%) as white plates: ^{1}H NMR ($CDCl_3$) δ 7.42 (d, $J = 8.8$ Hz, 4H), 7.06 (d, $J = 8.8$ Hz, 4H), 1.44 (s, 9H); ^{13}C NMR ($CDCl_3$) δ 152.99, 141.61, 131.84, 128.38, 119.21, 81.94, 28.25. Anal. Calcd for $C_{17}H_{17}N_1O_2Br_2$: C, 47.80; H, 4.01; N, 3.28; O, 7.49; Br, 37.41. Found: C, 47.55; H, 3.86; N, 3.13; O, 7.45; Br, 37.23.

Di-4-anisylamine (5). 4-Iodoanisole (8.43 g, 36.0 mmol), *p*-acetanisidide (4.96 g, 30.0 mmol), CuI (0.27 g, 1.4 mmol), and K_2CO_3 (10.4 g, 75.0 mmol) were heated together at 200 °C for 7 days with stirring under nitrogen atmosphere. After cooling, the reaction mixture was poured into dichloromethane, and inorganic residue was filtered off. Evaporation of the solvent afforded the crude oily mixture containing *N*-acetyl di-4-anisylamine, and this crude aniline was dissolved in methanol (150 mL). A large excess of KOH was added, and the resulting solution was heated to reflux for 12 h with stirring. After the solution was cooled to 0 °C, brown flakes were precipitated. Recrystallization of the flakes from hexane/ethyl acetate afforded pure **5** (4.74 g, 69%) as pale brown needles: ^{1}H NMR (acetone-d_6) δ 6.97 (d, $J = 8.8$ Hz, 4H), 6.82 (d, $J = 8.8$ Hz, 4H), 6.73 (s, 1H), 3.73 (s, 6H); ^{13}C NMR (acetone-d_6) δ 154.54, 139.20, 119.44, 115.23, 55.67. Anal. Calcd for $C_{14}H_{15}N_1O_2$: C, 73.34; H, 6.59; N, 6.11; O, 13.96. Found: C, 73.46; H, 6.47; N, 5.83; O, 13.89.

SCHEME 2: Preparation of the Dendritic Oligoarylamine 2

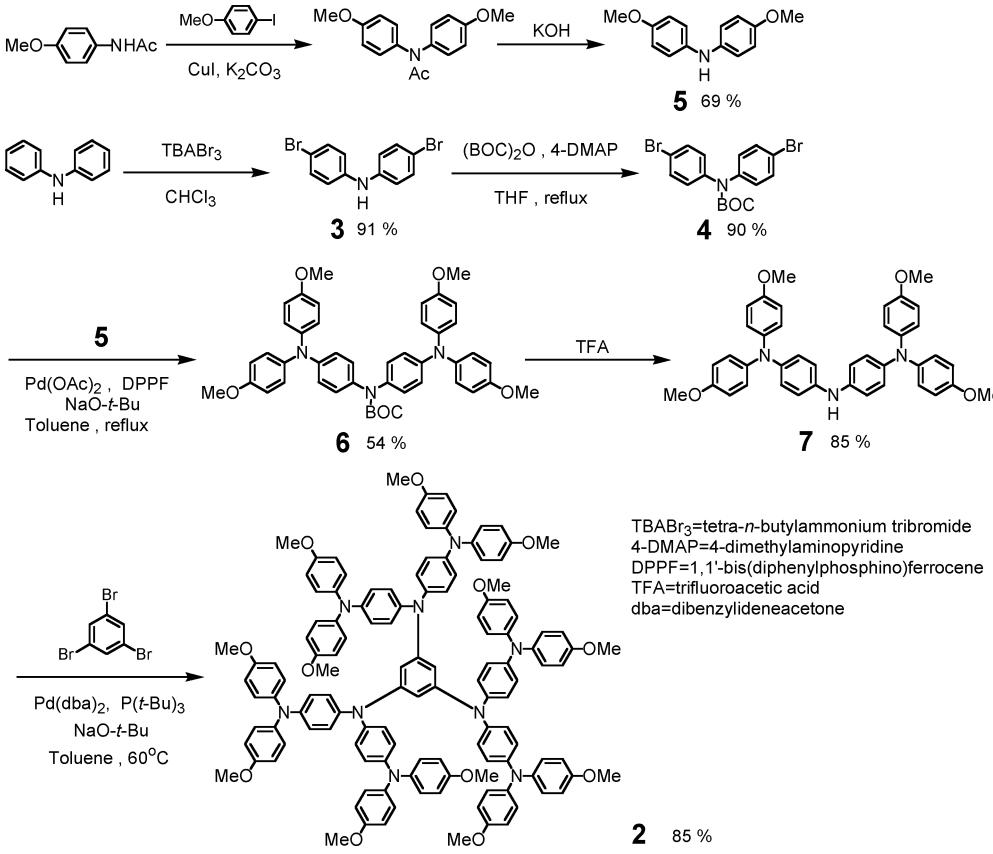

***N*-*tert*-Butoxycarbonyl-*N*,*N*-bis[4-(di-4-anisylamino)phenyl]amine (6).** Dibrominated arylamine **4** (0.99 g, 2.3 mmol), di-4-anisylamine **5** (1.59 g, 6.93 mmol), sodium *tert*-butoxide (0.78 g, 8.1 mmol), $Pd(OAc)_2$ (31.9 mg, 0.517 mmol), and 1,1′-bis-(diphenylphosphanyl)ferrocene (DPPF) (153 mg, 0.277 mmol) were dissolved in toluene (30 mL) in a Schlenk flask under argon. The reaction mixture was heated to reflux for 120 h with stirring. The mixture was washed with water and then dried over $MgSO_4$. After evaporation of solvent, flash column chromatography on silica gel with 7:3 dichloromethane/toluene afforded pure **6** (0.90 g, 54%) as a white solid: ^{1}H NMR (acetone-d_6) δ 7.07 (d, J = 8.8 Hz, 4H), 7.03 (d, J = 8.8 Hz, 8H), 6.89 (d, J = 8.8 Hz, 8H), 6.81 (d, J = 8.8 Hz, 4H), 3.78 (s, 12H), 1.42 (s, 9H); ^{13}C NMR (acetone-d_6) δ 157.00, 154.48, 147.30, 141.67, 137.08, 128.44, 127.31, 121.00, 115.56, 80.51, 55.66, 28.37. Anal. Calcd for $C_{45}H_{45}N_3O_6$: C, 74.67; H, 6.27; N, 5.81; O, 13.26. Found: C, 74.41; H, 6.40; N, 5.68; O, 13.30.

***N*,*N*-Bis[4-(di-4-anisylamino)phenyl]amine (7).** *tert*-Butoxycarbonyl (BOC)-protected oligoarylamine **6** (1.42 g, 1.97 mmol) was dissolved in trifluoracetic acid (TFA) (50 mL), and the reaction mixture was stirred at room temperature for 10 min. The resulting mixture assumed an intense deep-green color. After evaporation of TFA, toluene was added to the residue, then the mixture was washed with saturated aqueous solution of NaOH and dried over $MgSO_4$. The toluene solution turned yellow-green meanwhile. Evaporation of solvent and recrystallization from hexane/toluene afforded pure **7** (1.04 g, 85%) as a white solid: ^{1}H NMR (acetone-d_6) δ 7.11 (s, 1H), 6.99 (d, J = 8.8 Hz, 4H), 6.94 (d, J = 8.8 Hz, 8H), 6.87 (d, J = 8.8 Hz, 4H), 6.84 (d, J = 8.8 Hz, 4H), 3.76 (s, 12H); ^{13}C NMR (acetone-d_6) δ 155.91, 142.63, 142.18, 139.93, 125.45, 125.15, 118.93, 115.25, 55.63. Anal. Calcd for $C_{40}H_{37}N_3O_4$: C, 77.02; H, 5.98; N, 6.74; O, 10.26. Found: C, 77.11; H, 6.18; N, 6.52; O, 10.09.

***N*,*N*,*N*′,*N*′,*N*′′,*N*′′-Hexakis[4-(di-4-anisylamino)phenyl]-1,3,5-benzenetriamine (2).** A mixture of $Pd(dba)_2$ (91.8 mg, 0.159 mmol) and tri-*tert*-butylphosphine (25.8 mg, 0.128 mmol) in toluene (20 mL) was stirred under argon at room temperature for 5 min. In a Schlenk flask under argon were placed oligoarylamine **7** (0.75 g, 1.2 mmol), 1,3,5-tribromobenzene (0.08 g, 0.2 mmol), and sodium *tert*-butoxide (0.14 g, 1.5 mmol). To this Schlenk flask, the above Pd catalyst solution was added via a syringe, and the solution was heated to 60 °C for 120 h with stirring. After cooling, the mixture was washed with water and dried over $MgSO_4$. After evaporation of solvent, flash column chromatography on basic alumina with 7:2:1 toluene/hexane/ethyl acetate and recrystallization from hexane/toluene afforded pure **2** (0.40 g, 85%) as a white solid: ^{1}H NMR ($CDCl_3$) δ 6.96 (d, J = 8.8 Hz, 24H), 6.87 (d, J = 8.8 Hz, 12H), 6.79 (d, J = 8.8 Hz, 12H), 6.73 (d, J = 8.8 Hz, 24H), 6.26 (bs, 3H), 3.73 (s, 36H). Anal. Calcd for $C_{126}H_{111}N_9O_{12}$: C, 77.88; H, 5.76; N, 6.49; O, 9.88. Found: C, 77.92; H, 5.80; N, 6.20; O, 9.59; FABMS m/z ($M - H^+$) calcd 1942.3, obsd 1942.

$2^{3+}(SbCl_6^-)_3$. In a 300 mL round-bottom flask under nitrogen atmosphere was placed tris(4-bromophenyl)aminium hexachloroantimonate (49.1 mg, 0.0601 mmol). This flask was then cooled to 195 K, and the solution of **2** (35.5 mg, 0.0183 mmol) in dry dichloromethane (2.5 mL) was added with stirring. At this time, dry *n*-butyronitrile (0.5 mL) was added slowly, and the mixture was then allowed to stir for 20 min at 195 K. The solution turned deep green. After stirring, dry ether (150 mL) was added, and a portion of precipitate was observed. The solution was then warmed slowly to room temperature for 20 min. The precipitates were grown into bulky ones and gathered by suction filtration. After washing with dry ether, the green solid was collected and dried under high vacuum for 24 h (42.7

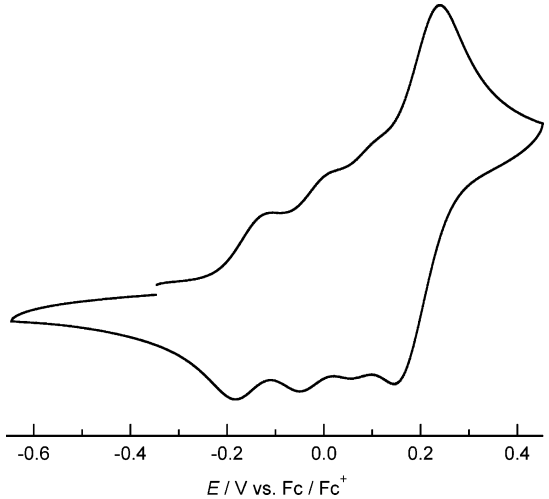

Figure 3. Cyclic voltammogram of **2** in benzonitrile at room temperature with scan rate of 100 mV/s.

TABLE 1: Redox Potentials (vs Fc/Fc$^+$) of 1 and 2 in Benzonitrile at Room Temperature

	E_1^0 (V)	E_2^0 (V)	E_3^0 (V)	E_4^0 (V)
1	−0.29	−0.13	−0.02	0.20[a]
2	−0.14	−0.01	+0.09	0.19[a]

[a] Quasi-three-electron oxidation.

mg, 79%). Anal. Calcd for $C_{126}H_{111}N_9O_{12}Sb_3Cl_{18}$: C, 51.36; H, 3.80; N, 4.28. Found: C, 51.12; H, 3.91; N, 4.13.

Results and Discussion

Synthesis. The dendritic oligoarylamine **2** was prepared via the sequential palladium-catalyzed amination reactions as shown in Scheme 2. Treatment of diphenylamine with tetrabutylammonium tribromide ($TBABr_3$) gave the dibrominated diphenylamine **3** in 91% yield.[25]

After protection of the secondary amino group of **3** with the *tert*-butoxycarbonyl (BOC) group,[26] BOC-protected triamine **6** was generated from the BOC-protected di(4-bromophenyl)amine **4** and di(4-anisyl)amine **5** in the presence of $Pd(OAc)_2$ and 1,1′-bis-(diphenylphosphanyl)ferrocene (DPPF),[22] and then was deprotected to yield triamine **7** with trifluoroacetic acid (TFA).[27,28] Finally, palladium-catalyzed ($Pd(dba)_2$ and P(*t*-Bu)$_3$) condensation of 1,3,5-tribromobenzene with triamine **7** afforded the target compound **2** in 85% yield.[22,29]

Electrochemistry. The electrochemical property of **2** was examined by cyclic voltammetry at room temperature. The redox potentials were determined in benzonitrile with 0.1 M tetrabutylammonium perchlorate as a supporting electrolyte. The cyclic voltammogram of **2** is shown in Figure 3, and the observed redox potentials are summarized in Table 1 together with those of **1** measured under the same conditions. First of all, the cyclic voltammogram of **2** revealed four reversible redox couples, and its behavior is similar to that of **1**. This result indicates that the higher oxidation state up to hexacation is accessible also to **2**. The observed oxidation peak current for the fourth oxidation wave is almost three times as large as those for the first three oxidation waves. In this view, each of the first three oxidation processes can be considered as one-electron transfer from each of the peripheral three oligoarylamine moieties, and the fourth oxidation process corresponds to the quasi-three-electron oxidation from the semi-quinone radical cation of the peripheral three oligoarylamine moieties. Moreover, each oxidation potential of **2** shifts generally higher as compared to the corresponding value of **1**. This tendency is simply attributable to the substituent effect at the periphery of **2**. The decrease in electron-donating ability of **2** can be caused by the replacement of the dimethylamino groups of **1** by the weak electron-withdrawing dianisylamino groups.

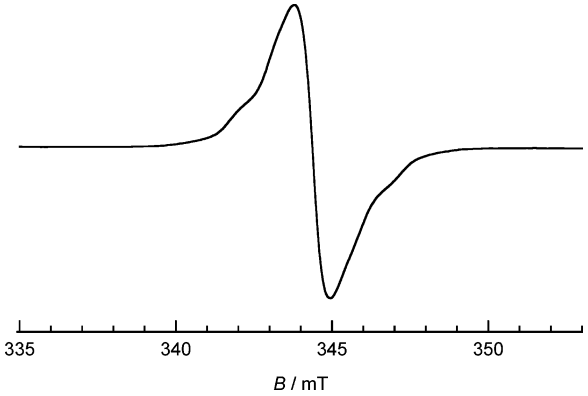

Figure 4. ESR spectrum of **2** at 123 K after addition of 1 equiv of oxidant.

ESR Measurements. In the same manner as the case of **1**, each oxidation state of the dendritic oligoarylamine **2** was generated by the stepwise chemical oxidation with tris(4-bromophenyl)aminium hexachloroantimonate ($TBA{\cdot}SbCl_6$) at 195 K in *n*-butyronitrile. To determine the definite spin multiplicity of the oxidized species, and to overcome the obscure continuous wave (CW) ESR spectrum originating from the existence of the paramagnetic species with different spin multiplicities, we carried out the electron spin transient nutation (ESTN) measurements in addition to the conventional CW-ESR measurements. The ESTN method is one of the pulsed-ESR techniques[30] and is based on the fact that the magnetic moments with different spin multiplicity process with their specific nutation frequency (ω_n) in the presence of a microwave irradiation field and a static magnetic field. If the microwave irradiation field is weak enough compared to the fine-structure parameter, the nutation frequency for the $|S, M_S\rangle \Leftrightarrow |S, M_S - 1\rangle$ allowed transition is given in a good approximation, by

$$\omega_n = [S(S+1) - M_S(M_S-1)]^{1/2}\omega_1 \qquad (1)$$

This equation indicates that the nutation frequency ω_n can be scaled with the spin quantum numbers S and M_S in a unit of ω_1, the nutation frequency for the doublet state. Thus, the nutation frequency can be regarded as a useful quantity to determine the definite spin multiplicity of the high-spin species existing in the oxidized solution.[16d,f,20]

When less than 1 molar equiv of oxidant was added to a solution of **2** (1 mM), a strong single line ESR signal with only poorly resolved hyperfine structures was observed at $g = 2.0033$ at 123 K (Figure 4). Furthermore, the resonance for the $\Delta M_S = \pm 2$ forbidden transition was not observed at the half-field region (∼170 mT). Hence, the observed ESR spectrum gives the evidence that the generated oxidized species is a spin-doublet radical cation.

On the other hand, the ESR spectrum of **2** oxidized with 2 molar equiv of oxidant showed a definite fine-structured pattern characteristic for spin-triplet species at 80 K (Figure 5). The central small signal can be ascribed to the existence of doublet species of $\mathbf{2}^+$. In addition, $\Delta M_S = \pm 2$ forbidden transition was also detected at the half-field region (∼170 mT). This indicates the presence of high-spin species in the oxidized solution. To identify the spin multiplicity of the high-spin components, we

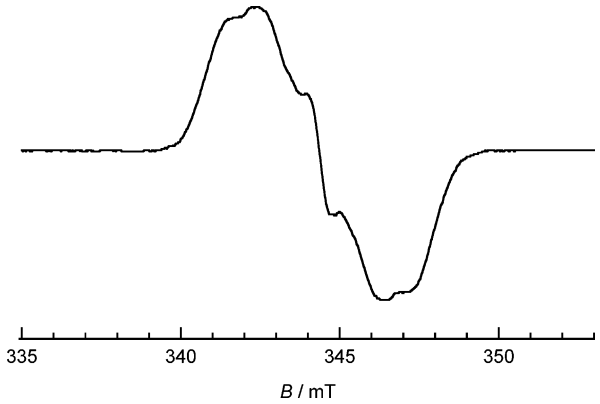

Figure 5. ESR spectrum of **2** at 80 K after addition of 2 equiv of oxidant.

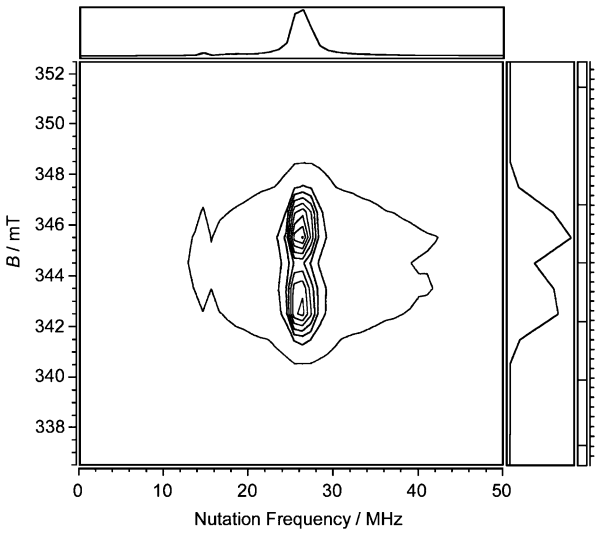

Figure 6. 2D ESTN spectra of **2** at 80 K after addition of 2 equiv of oxidant.

carried out the ESTN measurement at 80 K. From the 2D contour plot (Figure 6), the intense peaks were observed at 342.7 and 345.6 mT having the same nutation frequency (26.0 MHz). These two peaks are ascribed to the $|1, 0\rangle \leftrightarrow |1, \pm 1\rangle$ allowed transitions for the spin-triplet state. This assignment is confirmed by the absence of the other nutation frequency peaks assignable to the different spin states. From eq 1, if the high-spin species larger than $S = 1$ were present, the additional $\Delta M_S = \pm 1$ transitions should be observed. More noteworthy is the weakness of the nutation frequency peak for the doublet species of $\mathbf{2}^+$. This means the successful two-electron oxidation of **2**. Consequently, it can be concluded that the triplet $\mathbf{2}^{2+}$ is the major component at this oxidation state. The zero-field splitting parameter $|D|$ from the dipolar electron−electron interaction was determined to be 2.78 mT (0.0026 cm^{-1}) from the peak-to-peak line width of *Z*-axis components in the CW-ESR spectrum of $\mathbf{2}^{2+}$.[31] The value of $|D|$ corresponds to an average distance of about 10.0 Å between two radical spin centers under the point dipole approximation.[32] This value is larger than the N1−N2 distance (4.89 Å) determined by the semiempirical MO (MNDO AM1) calculations for the D_3 symmetrical model compound of **2** without all the methoxy groups.[33] Rather, it takes an intermediate value between the N3−N4 distance (7.82 Å) and the N3−N5 distance (12.15 Å). Here, the atom numbering is shown in Scheme 1. With these results taken into account, the spectrum for this triplet state can be originated from the dipole−dipole interaction between two spins delocalized over the different peripheral oligoarylamine moieties.

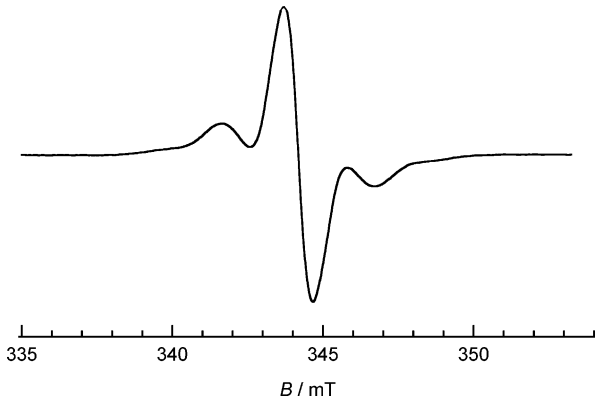

Figure 7. ESR spectrum of **2** at 80 K after addition of 3 equiv of oxidant.

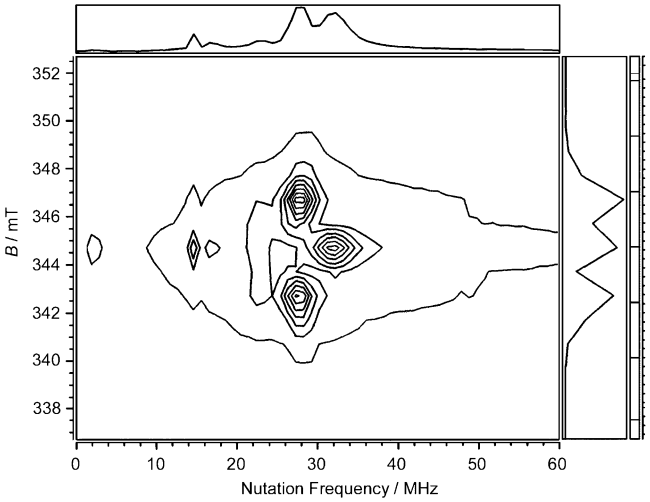

Figure 8. 2D ESTN spectra of **2** at 80 K after addition of 3 equiv of oxidant.

When treated with greater than 2 equiv of oxidant, the ESR spectrum changed gradually into a new five-line pattern spectrum shown in Figure 7, and this spectral change was completed just before the addition of 3 equiv of oxidant. The $\Delta M_S = \pm 2$ forbidden transition continued to be observed in the meantime. From the ESTN measurement on **2** at 80 K, the 2D contour plot of the ESTN spectra showed the intense nutation frequency peaks at 27.8 and 32.1 MHz (Figure 8). A frequency ratio of 32.1/27.8 corresponds to that of $2/\sqrt{3}$, which is calculated by $\omega_n = \sqrt{3}\ \omega_1$ for the $|^3/_2, \pm^3/_2\rangle \leftrightarrow |^3/_2, \pm^1/_2\rangle$ transitions and $\omega_n = 2\ \omega_1$ for the $|^3/_2, {}^1/_2\rangle \leftrightarrow |^3/_2, -^1/_2\rangle$ transition from eq 1. Hence, the nutation frequency peaks 27.8 and 32.1 MHz are attributable to the $|^3/_2, \pm^3/_2\rangle \leftrightarrow |^3/_2, \pm^1/_2\rangle$ and $|^3/_2, {}^1/_2\rangle \leftrightarrow |^3/_2, -^1/_2\rangle$ transitions for the spin-quartet state, respectively. It should be noted again that the other remarkable nutation frequency peaks than those corresponding to the spin quartet state were not seen in the spectrum. In conclusion, it can be deduced that the spin quartet $\mathbf{2}^{3+}$ is the major component in this oxidation state. The $|D|$ value of $\mathbf{2}^{3+}$ is determined to be 2.12 mT (0.0020 cm^{-1}). This value is smaller than the 3.00 mT (0.0028 cm^{-1}) observed for $\mathbf{1}^{3+}$. The decrease in the $|D|$ value means an increase in the average distance between three spin centers. This closely relates to the expansion of π-conjugation directing to the periphery of **2**. The extended π-system allows delocalization of spin density into the periphery and consequently results in relaxation of the Coulomb repulsion interaction.

Stability of Tricationic Species. The polycationic species of **2** were found to be far more stable than those of **1**. For

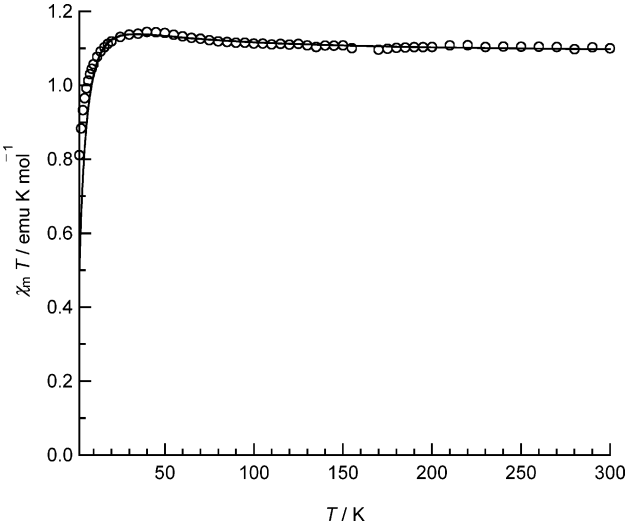

Figure 9. Temperature dependence of $\chi_m T$ of $\mathbf{2}^{3+}(SbCl_6^-)_3$ under a magnetic field of 500 G (open circle). The solid line represents the best theoretical fit to the data (see eqs 3−5).

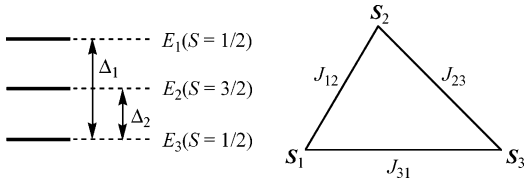

Figure 10. Energy level diagram for the two spin doublet states and the one spin quartet state originating from the magnetic interaction of a three-spin system, $S_1 = S_2 = S_3 = {}^1/_2$.

instance, the cationic species $\mathbf{2}^{2+}$ and $\mathbf{2}^{3+}$ in *n*-butyronitrile solution were stable under anaerobic condition at room temperature for days to weeks, as indicated by no loss in the ESR signal intensity. However, the lifetime of $\mathbf{1}^{2+}$ and $\mathbf{1}^{3+}$ in solution was considerably short at room temperature. In particular, we were able to isolate $\mathbf{2}^{3+}$ as $SbCl_6^-$ salts by the chemical oxidation with TBA·$SbCl_6$. Moreover, the ESR spectrum of the redissolved $\mathbf{2}^{3+}(SbCl_6^-)_3$ salts showed the same one of $\mathbf{2}^{3+}$ generated freshly in *n*-butyronitrile solution. This stability of $\mathbf{2}^{2+}$ and $\mathbf{2}^{3+}$ can be connected to the delocalization of spin distribution due to the extended π-conjugation and to the protection of the generated spins by the peripheral bulky groups.

Magnetic Properties of Tricationic Salts. The magnetic susceptibility of the powder sample of the $\mathbf{2}^{3+}(SbCl_6^-)_3$ salts was measured on a SQUID magnetometer in the temperature range 2−300 K at a constant field of 500 G. The temperature dependence of the molar magnetic susceptibility (χ_m) is shown in Figure 9. The $\chi_m T$ value of 1.10 emu K mol^{-1} at 300 K was close to the theoretical value of 1.125 emu K mol^{-1} for isolated three ${}^1/_2$ spins. Furthermore, the $\chi_m T$ value increased gradually with decreasing temperature and finally reached a maximum value of 1.14 emu K mol^{-1} at 40 K, indicating the intramolecular ferromagnetic interaction between three spins distributed over three peripheral oligoarylamine moieties. On the other hand, the $\chi_m T$ value dropped dramatically at very low temperature. The decrease in $\chi_m T$ value is indicative of the intermolecular antiferromagnetic interaction.

To understand the intramolecular magnetic interactions of $\mathbf{2}^{3+}$ quantitatively, we carried out the fitting of the temperature dependence of the magnetic susceptibility about $\mathbf{2}^{3+}(SbCl_6^-)_3$ salt. As shown in Figure 10, the interacting three-spin system can be represented by a triangular scheme, where each side of a triangle stands for the strength of the exchange coupling parameter J_{ij} between two spin centers $\boldsymbol{S}_i$ and $\boldsymbol{S}_j$. In this case, the spin Hamiltonian can be written by eq 2.

$$H = -2(J_{12}\boldsymbol{S}_1\boldsymbol{S}_2 + J_{23}\boldsymbol{S}_2\boldsymbol{S}_3 + J_{31}\boldsymbol{S}_3\boldsymbol{S}_1) \quad (2)$$

Although we tried to fit the data to regular ($J_{12} = J_{23} = J_{31}$) and isosceles ($J_{12} = J_{23} \neq J_{31}$) triangular schemes, all trials have met with failure. Therefore, we used a general triangular scheme ($J_{12} \neq J_{23} \neq J_{31}$) expressed by eq 3,[34] where the energy differences between three spin states Δ_1 and Δ_2 are defined by eqs 4 and 5 (Figure 10). Here, we assume that the intermolecular magnetic interaction can be treated with a mean field theory (the Curie−Weiss rule). The purity factor f represents the paramagnetic purity of $\mathbf{2}^{3+}(SbCl_6^-)_3$ salt including all the other experimental errors. The other parameters, N_A, g, k_B, μ_B, and θ are the Avogadro number, the *g*-factor, the Boltzmann constant, the Bohr magneton, and the Weiss constant, respectively.

$$\chi_m T = f\frac{N_A g^2 \mu_B{}^2}{4k_B}\frac{1 + \exp(-\Delta_1/k_B T) + 10\exp(-\Delta_2/k_B T)}{1 + \exp(-\Delta_1/k_B T) + 2\exp(-\Delta_2/k_B T)}\frac{T}{T-\theta} \quad (3)$$

$$\Delta_1 = 2(J_{12}{}^2 + J_{23}{}^2 + J_{31}{}^2 - J_{12}J_{23} - J_{23}J_{31} - J_{31}J_{12})^{1/2} \quad (4)$$

$$\Delta_2 = \Delta_1/2 - (J_{12} + J_{23} + J_{31}) \quad (5)$$

Apparently, eqs 3−5 contain too many parameters to determine the three exchange coupling parameters J_{ij} uniquely. Then, we performed the least-squares fitting of the experimental data to eq 3 as a function of Δ_1 and Δ_2. As a result, the best fit parameters were found: $f = 0.96$, $\Delta_1 = 33.6$ K, $\Delta_2 = -9.5$ K, and $\theta = -5.3$ K. The negative value of Δ_2 indicates that the spin quartet state is the ground state of $\mathbf{2}^{3+}$ and that the energy difference between the quartet and the low-lying doublet state is 19 cal/mol. We could not obtain the single crystal of $\mathbf{2}^{3+}(SbCl_6^-)_3$ salt for X-ray crystallographical analysis. However, the fact that the three exchange coupling constants are different ($J_{12} \neq J_{23} \neq J_{31}$) is explainable on the grounds that the molecular structure of $\mathbf{2}^{3+}$ is somewhat distorted owing to the peripheral bulky substituents, and therefore, the trication has no C_2 and C_3 symmetry axes in the solid state.

Conclusions

We have synthesized the new dendritic oligoarylamine **2** by using the successive palladium-catalyzed amination reactions in order to improve the stability of the highly charged species of 1,3,5-triaminobenzene, which are one of the interesting and fundamental organic high-spin molecules, and to compare the electronic structures of $\mathbf{2}^{3+}$ with those of $\mathbf{1}^{3+}$, which was reported to be a less stable spin-quartet trication. Moreover, the bulky peripheral dianisylamino groups of **2** were expected to influence the molecular structure and the resulting electronic structures, as compared to the dimethylamino-substituted **1**.

From the electrochemical studies, the redox behavior of **2** is similar to that of **1**, and the reversible stepwise oxidation up to the hexacation was found to be possible also for **2**. The substituting effect was reflected on the oxidation potentials, which were somewhat higher than the corresponding ones observed in **1**, probably owing to the weak electron-withdrawing dianisylamino groups. Stepwise chemical oxidation with TBA·$SbCl_6$ generated mono-, di-, and trications of **2** with ease. The spin multiplicity of the major species was determined to be doublet, triplet, and quartet for one-, two-, and three-electron

oxidation of **2** from the CW and pulsed ESR measurements. In contrast to the case of **1**, the high-spin species was found to be dominant in the generated paramagnetic species, probably due to high stability of the oxidized species of **2** in solution. Furthermore, the radical spin in $\mathbf{2}^{2+}$ and $\mathbf{2}^{3+}$ was found to be delocalized over the peripheral dianisylamino groups due to extension of π-conjugation. The improvement of stability by introduction of the bulky dianisylamino groups and by the expansion of the π-conjugated system enabled us to prepare the isolable tricationic salt of **2** and to examine the magnetic interaction in trication $\mathbf{2}^{3+}$. The analysis of the temperature dependence of the magnetic susceptibility of the $\mathbf{2}^{3+}$ salt revealed that the ferromagnetic interaction exists between three spins in $\mathbf{2}^{3+}$. Moreover, it was suggested that the molecular structure of $\mathbf{2}^{3+}$ is deformed in the solid state to have different exchange coupling constants among three spin centers. This structural deformation can be ascribed to the bulky dianisylamino groups in $\mathbf{2}^{3+}$.

Acknowledgment. This work was supported by CREST (Core Research for Evolutional Science and Technology) of Japan Science and Technology Agency (JST) and by a Grant-in-Aid for Scientific Research from Japan Society for Promotion of Science (JSPS). Thanks are due to the Research Center for Molecular-Scale Nanoscience, the Institute for Molecular Science, for assistance in obtaining the pulsed ESR spectra. Numerical calculations were partly carried out at the Supercomputer Laboratory of the Institute for Chemical Research of Kyoto University.

References and Notes

(1) Shirota, Y. *J. Mater. Chem.* **2000**, *10*, 1−25, and references therein.
(2) Wu I.-Y.; Lin, J. T.; Tao Y.-T.; Balasubramaniam, E. *Adv. Mater.* **2000**, *12*, 668−669.
(3) Freeman, A. W.; Koene, S. C.; Malenfant, P. R. L.; Thompson, M. E.; Fréchet, J. M. J. *J. Am. Chem. Soc.* **2000**, *122*, 12385−12386.
(4) Li, J. C.; Kim, K.-Y.; Blackstock, S. C.; Szulczewski, G. J. *Chem. Mater.* **2004**, *16*, 4711−4714.
(5) (a) Bonvoisin, J.; Launay, J.-P.; van der Auweraer, M.; de Schryver, F. C. *J. Phys. Chem.* **1994**, *98*, 5052−5057; **1996**, *100*, 18006 (erratum). (b) Bonvoisin, J.; Launay, J.-P.; Verbouwe, W.; van der Auweraer, M.; de Schryver, F. C. *J. Phys. Chem.* **1996**, *100*, 17079−17082.
(6) (a) Lambert, C.; Nöll, G. *J. Am. Chem. Soc.* **1999**, *121*, 8434−8442. (b) Lambert, C.; Nöll, G.; Hampel, F. *J. Phys. Chem. A* **2001**, *105*, 7751−7758. (c) Lambert, C.; Nöll, G.; Schelter, J. *Nat. Mater.* **2002**, *1*, 69−73. (d) Lambert, C.; Nöll, G. *Chem.—Eur. J.* **2002**, *8*, 3467−3477. (e) Lambert, C.; Nöll, G.; Schelter, J. *J. Phys. Chem. A* **2004**, *108*, 6474−6486.
(7) Ranasinghe, M. I.; Varnavski, O. P.; Pawlas, J.; Hauck, S. I.; Louie, J.; Hartwig, J. F.; Goodson, T., III *J. Am. Chem. Soc.* **2002**, *124*, 6520−6521.
(8) (a) Selby, T. D.; Blackstock, S. C. *J. Am. Chem. Soc.* **1998**, *120*, 12155−12156. (b) Selby, T. D.; Kim, K.-Y.; Blackstock, S. C. *Chem. Mater.* **2002**, *14*, 1685−1690. (c) Kim, K.-Y.; Hassenzahl, J. D.; Selby, T. D.; Szulczewski, G. J.; Blackstock, S. C. *Chem. Mater.* **2002**, *14*, 1691−1694.
(9) Bronk, K.; Thayumanavan, S. *J. Org. Chem.* **2003**, *68*, 5559−5567.
(10) Yan, X. Z.; Pawlas, J.; Goodson, T., III *J. Am. Chem. Soc.* **2005**, *127*, 9105−9116.
(11) Lambert, C.; Schelter, J.; Fiebig, T.; Mank, D.; Trifonov, A. *J. Am. Chem. Soc.* **2005**, *127*, 10600−10610.
(12) (a) Yoshizawa, K.; Tanaka, K.; Yamabe, T. *Chem. Lett.* **1990**, 1331−1314. (b) Yoshizawa, K.; Takata, A.; Tanaka, K.; Yamabe, T. *Polym. J.* **1992**, *24*, 857−864. (c) Ito, A.; Ota, K.; Tanaka, K.; Yamabe, T.; Yoshizawa, K. *Macromolecules* **1995**, *28*, 5618−5625. (d) Yoshizawa, K.; Hoffman, R. *Chem.—Eur. J.* **1995**, *1*, 403−413.
(13) (a) Bushby, R. J.; Ng, K. M. *Chem. Commun.* **1996**, 659−660. (b) Bushby, R. J.; McGill, D. R.; Ng, K. M.; Taylor, N. *Chem. Commun.* **1996**, 2641−2642. (c) Bushby, R. J.; McGill, D. R.; Ng, K. M.; Taylor, N. *J. Mater. Chem.* **1997**, *7*, 2343−2354. (d) Bushby, R. J.; Gooding, D. *J. Chem. Soc., Perkin Trans. 2* **1998**, 1069−1075.
(14) (a) Baumgarten, M.; Müllen, K.; Tyutyulkov, N.; Madjarova, G. *Chem. Phys.* **1993**, *169*, 81−84. (b) Madjarova, G.; Baumgarten, M.; Müllen, K.; Tyutyulkov, N. *Makromol. Chem., Theory Simul.* **1994**, *3*, 803−815. (c) Tyutylkov, N.; Baumgarten, M.; Dietz, F. *Chem. Phys. Lett.* **2002**, *353*, 231−238.
(15) (a) Takahashi, M.; Nakazawa, T.; Tsuchida, E.; Nishide, H. *Macromolecules* **1999**, *32*, 6383−6385. (b) Michinobu, T.; Inui, J.; Nishide, H. *Org. Lett.* **2003**, *5*, 2165−2168.
(16) (a) Yoshizawa, K.; Chano, A.; Ito, A.; Tanaka, K.; Yamabe, T.; Fujita, H.; Yamauchi, J.; Shiro, M. *J. Am. Chem. Soc.* **1992**, *114*, 5994−5998. (b) Ito, A.; Taniguchi, A.; Yamabe, T.; Tanaka, K. *Org. Lett.* **1999**, *1*, 741−743. (c) Ito, A.; Ono, Y.; Tanaka, K. *Angew. Chem., Int. Ed.* **2000**, *39*, 1072−1075. (d) Ito, A.; Ino, H.; Tanaka, K.; Kanemoto, K.; Kato, T. *J. Org. Chem.* **2002**, *67*, 491−498. (e) Ito, A.; Urabe, M.; Tanaka, K. *Angew. Chem., Int. Ed.* **2003**, *42*, 921−924. (f) Ito, A.; Ino, H.; Matsui, Y.; Hirao, Y.; Tanaka, K. *J. Phys. Chem. A* **2004**, *108*, 5715−5720.
(17) (a) Stickly, K. R.; Blackstock, S. C. *J. Am. Chem. Soc.* **1994**, *116*, 11576−11577. (b) Stickly, K. R.; Selby, T. D.; Blackstock, S. C. *J. Org. Chem.* **1997**, *62*, 448−449. (c) Selby, T. D.; Blackstock, S. C. *J. Am. Chem. Soc.* **1999**, *121*, 7152−7153. (e) Selby, T. D.; Blackstock, S. C. *Org. Lett.* **1999**, *1*, 2053−2055. (f) Selby, T. D.; Stickly, K. R.; Blackstock, S. C. *Org. Lett.* **2000**, *2*, 171−174.
(18) (a) Wienk, M. M.; Janssen, R. A. J. *Chem. Commun.* **1996**, 267−268. (b) Wienk, M. M.; Janssen, R. A. J. *J. Am. Chem. Soc.* **1996**, *118*, 10626−10628. (c) Wienk, M. M.; Janssen, R. A. J. *J. Am. Chem. Soc.* **1997**, *119*, 4492−4501. (d) Struijk, M. P.; Janssen, R. A. J. *Synth. Met.* **1999**, *103*, 2287−2290. (e) van Meurs, P. J.; Janssen, R. A. J. *J. Org. Chem.* **2000**, *65*, 5712−5719.
(19) (a) Okada, K.; Imakura, T.; Oda, M.; Murai, H.; Baumgarten, M. *J. Am. Chem. Soc.* **1996**, *118*, 3047−3048. (b) Okada, K.; Imakura, T.; Oda, M.; Kajiwara, A.; Kamachi, M.; Sato, K.; Shiomi, D.; Takui, T.; Itoh, K.; Gherghel, L.; Baumgarten, M. *J. Chem. Soc., Perkin Trans. 2* **1997**, 1059−1060. (c) Kozaki, M.; Nakamura, S.; Sato, K.; Takui, T.; Kamatani, T.; Oda, M.; Tokumaru, K.; Okada, K. *Tetrahedron Lett.* **1998**, *39*, 5979−5982.
(20) Sato, K.; Yano, M.; Furuichi, M.; Shiomi, D.; Takui, T.; Abe, K.; Itoh, K.; Higuchi, A.; Katsuma, K.; Shirota, Y. *J. Am. Chem. Soc.* **1997**, *119*, 6607−6613.
(21) Bushby, R. J.; McGill, D. R.; Ng, K. M.; Taylor, N. *J. Chem. Soc., Perkin Trans. 2* **1997**, 1405−1414.
(22) Hauck, S. I.; Lakshmi, K. V.; Hartwig, J. F. *Org. Lett.* **1999**, *1*, 2057−2060.
(23) Michinobu, T.; Takahashi, M.; Tsuchida, E.; Nishide, H. *Chem. Mater.* **1999**, *11*, 1969−1971.
(24) Crayston, J. A.; Devine, J. N.; Walton, J. C. *Tetrahedron* **2000**, *56*, 7829−7857, and references therein.
(25) Berthelot, J.; Guette, C.; Essayegh, M.; Desbene, P. L.; Basserlier, J. J. *Synth.Commun.* **1986**, *16*, 1641−1645.
(26) Singer, R. A.; Sadighi, J. P.; Buchwald, S. L. *J. Am. Chem. Soc.* **1998**, *120*, 213-214.
(27) Schwyzer, R.; Costopanagiotis, A.; Sieber, P. *Helv. Chim. Acta* **1963**, *46*, 870−889.
(28) Sakai, N.; Ohfune, Y. *J. Am. Chem. Soc.* **1992**, *114*, 998−1010.
(29) Hartwig, J. F.; Kawatsura, M.; Hauck, S. I.; Shaughnessy, K. H.; Alcazar-Roman, L. M. *J. Org. Chem.* **1999**, *64*, 5575−5580.
(30) Astashkin, A. V.; Schweiger, A. *Chem. Phys. Lett.* **1990**, *174*, 595−602.
(31) Weltner, W., Jr. *Magnetic Atoms and Molecules*; Dover: New York, 1989.
(32) Hirota, N. *J. Am. Chem. Soc.* **1967**, *89*, 32−41.
(33) The *Gaussian 98* (revision A.9) program was used for the present MNDO AM1 calculations. As for the calculation method, see: Dewar, M. J. S.; Zoebisch, E. G.; Healy, E. F.; Stewart, J. J. P. *J. Am. Chem. Soc.* **1985**, *107*, 3902−3909.
(34) Sinn, E. *Coord. Chem. Rev.* **1970**, *5*, 313−347